Acknowledgments. We greatly appreciate support of this work by National Science Foundation Grant GP 31565-X. We also are grateful to Professors P. Kebarle, R. McIver, and F. G. Bordwell for sharing unpublished data with us and to Professor Hepler and referees for critical suggestions.

References and Notes

(1) L. P. Hammett, "Physical Organic Chemistry", 2d ed, McGraw-Hill, New York, N.Y., 1970.
(2) J. Hine, "Structural Effects on Equilibria in Organic Chemistry", Wiley, New York, N.Y., 1975.
(3) L. Hepler and J. Larson in "Solute-Solvent Interactions", J. F. Coetzee and C. D. Ritchie, Ed., Marcel Dekker, New York, N.Y., 1969; see also L. G. Hepler and E. M. Woolley in "Water", Vol. 3, F. Franks, Ed., Plenum Press, New York, N.Y., 1973, and P. D. Bolton and L. G. Hepler, *Q. Rev., Chem. Soc.*, **4**, 521 (1971).
(4) S. Ehrenson, *Prog. Phys. Org. Chem.*, **2**, 195 (1964).
(5) C. D. Ritchie and W. F. Sager, *Prog. Phys. Org. Chem.*, **2**, 323 (1964).
(6) N. B. Chapman and J. Shorter, Ed., "Advances in Linear Free Energy Relationships", Plenum Press, New York, N.Y., 1972.
(7) G. Kortüm, W. Vogel, and K. Andrussow, "Dissociation Constants of Organic Acids in Aqueous Solution", Butterworths, London, 1962.
(8) H. C. Brown, D. H. McDaniel, and O. Häfliger in "Determination of Organic Structures by Physical Methods", Academic Press, New York, N.Y., 1955.
(9) R. P. Bell, "The Proton in Chemistry,", 2d ed, Cornell University Press, Ithaca, N.Y., 1973.
(10) P. D. Bolton, K. A. Fleming, and F. M. Hall, *J. Am. Chem. Soc.*, **94**, 1033 (1972).
(11) L. P. Fernandez and L. G. Hepler, *J. Am. Chem. Soc.*, **81**, 1783 (1959).
(12) L. G. Hepler and W. F. O'Hara, *J. Phys. Chem.*, **65**, 811 (1961).
(13) W. F. O'Hara and L. G. Hepler, *J. Phys. Chem.*, **65**, 2107 (1961).
(14) T. Matsui, H. C. Ko, and L. G. Hepler, *Can. J. Chem.*, **52**, 2906 (1974).
(15) (a) C. L. Liotta, H. P. Hopkins, Jr., and P. T. Kasudia, *J. Am. Chem. Soc.*, **96**, 7153 (1974); (b) C. L. Liotta, Report on OWRR Project No. B-049-gA, July 1, 1970 to August 31, 1973.
(16) P. D. Bolton, C. H. Rochester, and B. Rossall, *Trans. Faraday Soc.*, **66**, 1348 (1970).
(17) P. D. Bolton, F. M. Hall, and I. H. Reece, *J. Chem. Soc. B*, 709 (1967).
(18) P. D. Bolton, F. M. Hall, and I. H. Reece, *J. Chem. Soc. B*, 717 (1966).
(19) R. A. Cox, A. M. Last, and R. Stewart, *J. Chem. Soc., Perkin Trans. 2*, 1678 (1974).
(20) G. H. Parsons and C. H. Rochester, *J. Chem. Soc., Faraday Trans. 1*, 1069 (1975).
(21) G. H. Parsons and C. H. Rochester, *J. Chem. Soc., Perkin Trans. 2*, 1313 (1974).
(22) G. H. Parsons, C. H. Rochester, and C. E. C. Wood, *J. Chem. Soc. B*, 533 (1971).
(23) C. H. Rochester and B. Rossall, *J. Chem. Soc. B*, 743 (1967).
(24) J. E. Leffler and E. Grunwald, *"Rates and Equilibria of Organic Reactions"*, Wiley, New York, N.Y., 1963.
(25) R. T. McIver, Jr., and J. H. Silvers, *J. Am. Chem. Soc.*, **95**, 8462 (1973).
(26) R. Yamdagni, T. B. McMahon, and P. Kebarle, *J. Am. Chem. Soc.*, **96**, 4035 (1974).
(27) E. M. Arnett, L. E. Small, R. T. McIver, Jr., and J. S. Miller, *J. Am. Chem. Soc.*, **96**, 5638 (1974).
(28) E. M, Arnett, D. E. Johnston, L. E. Small, and D. Oancea, *Faraday Symp. Chem. Soc.*, **No. 10** (1975).
(29) E. M. Arnett, D. E. Johnston, and L. E. Small, *J. Am. Chem. Soc.*, **97**, 5598 (1975).
(30) E. M. Arnett, T. C. Moriarity, L. E. Small, J. P. Rudolph, and R. P. Quirk, *J. Am. Chem. Soc.*, **95**, 1492 (1973).
(31) E. M. Arnett and L. E. Small, *J. Am. Chem. Soc.*, submitted for publication.
(32) E. M. Arnett, W. G. Bentrude, J. J. Burke, and P. M. Duggleby, *J. Am. Chem. Soc.*, **87**, 1541 (1965).
(33) J. D. Cox and G. Pilcher, "Thermochemistry of Organic and Organometallic Compounds", Academic Press, New York, N.Y., 1970.
(34) R. Dreisbach, *Adv. Chem. Ser.*, **No. 22** (1959); **No. 29** (1961).
(35) G. W. Thompson in "Technique of Organic Chemistry", Vol. I, 3d ed, A. Weissberger, Ed., Interscience, New York, N.Y., 1959.
(36) E. M. Arnett and D. Oancea, *J. Chem. Educ.*, 32, (1975).
(37) J. S. Chickos, *J. Chem. Educ.*, **52**, 134 (1975).
(38) C. V. Krishnan and H. L. Friedman, *J. Phys. Chem.*, **73**, 1572 (1969).
(39) R. S. Drago, M. S. Nozari, and G. C. Vogel, *J. Am. Chem. Soc.*, **94**, 90 (1972).
(40) M. S. Nozari, C. D. Jensen, and R. S. Drago, *J. Am. Chem. Soc.*, **95**, 3162 (1973).
(41) R. M. Guidry, and R. S. Drago, *J. Phys. Chem.*, **78**, 454 (1974).
(42) R. Fuchs and R. F. Rodewald, *J. Am. Chem. Soc.*, **95**, 5897 (1973).
(43) E. M. Arnett and J. F. Wolf, *J. Am. Chem. Soc.*, **97**, 3262 (1975).
(44) J. H. Hildebrand and R. L. Scott, "The Solubility of Nonelectrolytes", 3d ed, Reinhold, New York, N.Y., 1950.
(45) (a) C. H. Hansen and A. Beerbower, "Encyclopedia of Chemical Technology", 2d ed, Interscience, New York, N.Y., 1971; (b) M. R. J. Dack, *Chem. Soc. Rev.*, **4**, 211 (1975).
(46) M. Taagepera, W. G. Henderson, R. T. C. Brownlee, J. L. Beauchamp, D. Holtz, and R. W. Taft, *J. Am. Chem. Soc.*, **94**, 1369 (1972).
(47) J. Chaudhuri, J. Jagur-Grodzinski, and M. Szwarc, *J. Phys. Chem.*, **71**, 3063 (1967).
(48) J. I. Brauman and L. K. Blair, *J. Am. Chem. Soc.*, **92**, 5986 (1970).
(49) E. M. Arnett, F. M. Jones, III, M. Taagepera, W. G. Henderson, J. L. Beauchamp, D. Holtz, and R. W. Taft, *J. Am. Chem. Soc.*, **94**, 4724 (1972).
(50) D. H. Aue, H. M. Webb, and M. T. Bowers, *J. Am. Chem. Soc.*, **94**, 4726 (1972.
(51) J. F. Wolf, P. G. Harch, and R. W. Taft, *J. Am. Chem. Soc.*, **97**, 2904 (1975).
(52) C. D. Ritchie in "Solute-Solvent Interactions", C. D. Ritchie and J. F. Coetzee, Ed., Marcel Dekker, New York, N.Y., 1969.
(53) F. G. Bordwell, J. E. Bartmess, G. E. Drucker, Z. Margolin, and W. S. Matthews, *J. Am. Chem. Soc.*, **97**, 3226 (1975).
(54) P. H. Weiner, *J. Am. Chem. Soc.*, **95**, 5845 (1973).
(55) E. M. Arnett, E. J. Mitchell, and T. S. S. R. Murty, *J. Am. Chem. Soc.*, **96**, 3875 (1974).
(56) C. Tanford, "The Hydrophobic Effect", Wiley-Interscience, New York, N.Y., 1973.
(57) E. M. Arnett and D. R. McKelvey in "Solute-Solvent Interactions", C. D. Ritchie and J. F. Coetzee, Ed., Marcel Dekker, New York, N.Y., 1969.

Immobilized Radicals. 2. Hydrogen Bonding of the Semiquinone Anion Radical[1]

Brian J. Hales

Contribution from the Department of Chemistry, Louisiana State University, Baton Rouge, Louisiana 70803. *Received February 5, 1976*

Abstract: The ESR spectra of semiquinones in rigid alcohol solvents are broadened by radical-solvent interactions. These interactions are interpreted to be hydrogen bonds between the solvent's hydroxyl proton and the semiquinone's phenolate oxygen. Combined analysis of the change of the spectrum's line width and second moment as a function of the percentage of deuteration of the medium shows that one hydrogen bond occurs at each phenolate oxygen with a bond angle near 180°. Also shown by this analysis is the preference of hydrogen bonding of protons over deuterons in these systems.

It is customary in interpreting ESR spectra of organic radicals in solution to always consider the influence of solvent-radical interactions. These interactions manifest themselves as ion pairing, radical-solvent complex formation, secondary solvent radical production, hydrogen bonding, and polarity effects. All of these interactions affect the observed ESR spectrum, the magnitude of which can be as subtle as a small shift of the hyperfine splitting constants and the isotropic *g* factor or as pronounced as the incorporation of additional hyperfine splittings or even secondary radical signals. No matter what the magnitude of the effect, however, a radical's spectrum in the presence of these interactions will be different from that obtained for the isolated radical. Because of this, the solution spectrum often can be used as a monitor of the degree and type of radical–solvent interactions.

This paper represents the second in a series[1b] of articles on the use of paramagnetic species indigenous to living systems (i.e., biological radicals used as natural spin labels) as a probe of the species environment. Since these radicals are often bound to proteins or membranes, they commonly exhibit powder spectra associated with an immobilized radical. Unfortunately, powder spectra often have much less structure and are, therefore, more difficult to interpret than solution spectra. In spite of this frequent difficulty in interpretation, the interactions experienced by radicals in solution can be experienced similarly by immobilized radicals and, correspondingly, can have just as great an effect on perturbing powder spectra. Because of this, the perturbed powder spectrum can be used also to monitor an immobilized radical's environment. Such a monitor would greatly aid our probing living systems. This article will discuss one class of interactions, the effect of hydrogen bonding on the power spectrum of the p-benzosemiquinone anion radical.

The investigation of the effect of hydrogen bonding on the spectrum of the semiquinone anion of p-benzoquinone and its deuterated analogue has been undertaken in rigid alcohol solution. Unlike the spectrum observed in solution, the semiquinone in rigid media experiences hydrogen bonding strong enough to produce an observable broadening of its powder spectrum. This broadening is theorized to be due to a dipole-dipole interaction of the semiquinone's unpaired electron with the alcohol's hydroxyl proton via hydrogen bonding in the system.

The effect was first observed by Harbour and Tollin[2] while investigating the photochemical reaction of chlorophyll with quinone in alcohol solutions at low temperatures. They hypothesized that the broadening was due to the spectral overlap of the signals of a semiquinone and solvent radical, both of which are intermediates in the photochemical reaction. Using X- and Q-band ESR spectroscopy, we have demonstrated the existence of only a single radical species, i.e., the semiquinone anion. The geometry and structure of this radical–solvent complex have been inferred from spectra of it in both mixed deuterated and protonated solvents as well as solvents which have been selectively deuterated at the various hydrogen position. As expected, these studies show that the semiquinone is hydrogen bonded to the hydroxyl group of the alcohol. Also shown by these studies is a marked preference for hydrogen bonding with protonated solvents compared to deuterated solvents. The equilibrium constant for this competition of hydrogen bonding in methanol at temperatures just above the freezing point has been determined to be 5.8 and shown to correspond to the presence of two equivalent sites of bonding on the semiquinone in rigid media. Both the equilibrium constant and the number of hydrogen bonding sites can be unequivocally assigned using a unique technique of noting the variation in spectral line width and second moment as a function of the fraction of deuteration of the solvent and comparing these values with those calculated from different theoretical models.

Experimental Section

The semiquinone anion was generated by air oxidation[3] of the quinol in methanol containing 10^{-4} M NaOH. p-Benzoquinol (Allied) was used without further purification. Perdeuteriobenzoquinol was synthesized using the procedure of Charney and Becker.[4] Methanol (Aldrich, Reagent), methanol-d, and methanol-d_4 (Biorad, 99% purity) were used as received. All samples were cooled to near freezing then frozen to a rigid glass with liquid nitrogen prior to their incorporation into the resonance cavity of the ESR spectrometer.

X-band spectra were recorded on a JEOL spectrometer (JWS-3BS-X) equipped with a 12 in. magnet, while Q-band spectra were recorded on a modified Varian spectrometer (V-4500). Each spectrometer employed a cylindrical cavity resonating in the TE_{011} mode. Magnetic field intensities were measured with a Magnion Gaussmeter (G-504).

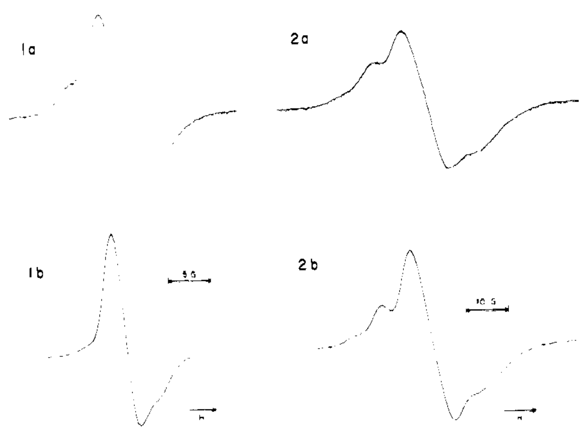

Figure 1. X-band (9.2 GHz) ESR spectra of deuterated (1) and protonated (2) p-benzosemiquinone anion in methanol (a) and methanol-d_4 (b) at 77 K. (Microwave power = 0.1 mW.)

Spectral amplitudes were digitized using a Calma Corp. tracing board interfaced with a Data General Mini-Computer. Second moments were calculated also by the Mini-Computer from the amplitude data. Due to the large error associated with the difficulty of manually digitizing data, second moments described in this paper represent the average of at least four determinations. The method used to simulate spectra has been described previously.[1b]

Results

The spin Hamiltonian of a free radical in an external magnetic field contains isotropic and anisotropic terms for both the hyperfine coupling and Zeeman interactions. In solvents of low viscosity the anisotropic interactions average out so that one only observes the radical's isotropic interactions in the ESR spectrum. As the temperature is lowered, however, the viscosity and rotational correlation time increase and the anisotropic components become observable, often broadening the spectrum to many times that of the isotropic spectrum. Such is the case of the benzosemiquinone anion, where freezing of this radical yields a single-lined, almost structureless powder spectrum compared to the normally well-resolved five-line spectrum at room temperature. Hales and Bolton[5] showed that the shape of this powder spectrum was unaffected when the radical was frozen into different protonated alcohol solvents. Harbour and Tollin[2] subsequently demonstrated that the semiquinone's power spectrum was affected dramatically, however, when deuterated alcohols were substituted for protonated alcohols.

Figure 1 shows the powder spectra of the normal benzosemiquinone anion and its fully deuterated analogue in methanol and methanol-d_4, recorded at X-band frequencies (9.2 GHz). For both radical species the powder spectrum is narrowed markedly in the deuterated solvent compared to the protonated solvent. Harbour and Tollin[2,6] suggested that the broadening was due to the presence of a solvent radical generated simultaneously with the semiquinone and frozen into the solvent matrix before it could decay by disproportionation. There are several lines of evidence arguing against this explanation. (1) The same powder spectrum is observed[1b] for the radical generated by photochemical, electrochemical, or chemical means. It is difficult to rationalize the simultaneous production of the same solvent radical in all these systems. (2) In our research the semiquinone was generated at room temperature then frozen to 77 K and not generated directly into the frozen alcohol matrix. The rate of disproportionation of

Table I. Spectral Parameters of Deuterated *p*-Benzosemiquinone Anion at 77 K

Solvent	Cation	g^{xx} [a]	g^{yy}	g^{zz}	$\langle H^2\rangle_{\mathrm{rel}}$ [b]
CH_3OH	Na^+	2.0062	2.0046	2.0023	3.0 ± 0.4
CH_3OD	Na^+	2.0065	2.0052	2.0023	2.1 ± 0.2
CD_3OD	Li^+	2.0065	2.0053	2.0023	1.0
CD_3OD	Na^+	2.0065	2.0053	2.0023	1.0
CD_3OD	K^+	2.0065	2.0053	2.0023	1.0
(Theoretical ref 1b		2.0059	2.0037	2.0023	

[a] All *g* factors ±0.0001. [b] Relative second moment based on $\langle H^2\rangle$ for radical in CD_3OD defined to equal unity.

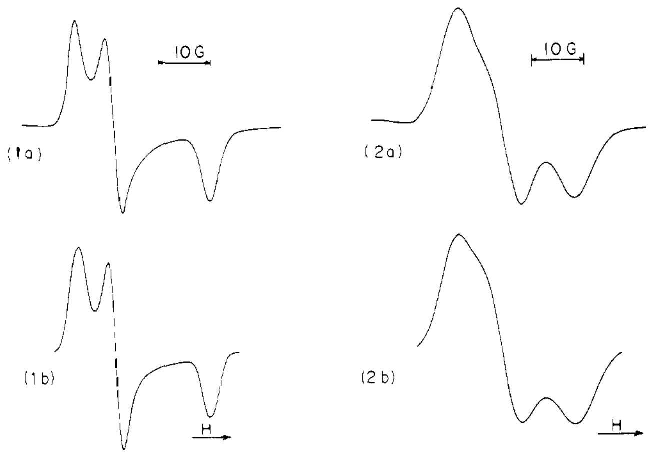

Figure 2. Experimental (a) and computer-simulated (b) ESR spectra of the fully deuterated semiquinone anion at Q-band (35 GHz) in methanol-d_4 (1) and methanol (2) at 77 K. (Microwave power = 0.1 mW.)

the solvent radical would be expected to be fast enough to render it undetectable by the time the system is frozen. This argument is strengthened by the fact that only the slower decaying semiquinone is observed in these systems at room temperature. Furthermore, if the frozen samples are thawed and then refrozen, the same powder spectrum is observed. (3) If all of the spectra in Figure 1 represented the spectral overlap of two different signals, deuteration of one or both species should allow a separation or enhanced resolution of the underlying signals. In fact, solvent deuteration only narrows the semiquinone's spectrum uniformly both for the protonated and deuterated quinone. Such a uniform spectral narrowing cannot be explained in terms of overlapping spectra.

This narrowing effect is better observed at Q-band (35 GHz) frequencies. Overlapping signals with different principal *g* factors are further separated and, therefore, better resolved at Q- compared to X-band frequencies. Figure 2 shows the spectrum of immobilized deuterated semiquinone in both protonated and deuterated methanol. This figure clearly shows that this powder spectrum is due to only one radical species, the semiquinone anion, and that deuteration of the solvent has the sole effect of uniformly narrowing the spectrum of that species. Computer simulations of these spectra yield the principal *g* factors listed in Table I along with their calculated second moments ($\langle H^2\rangle$). The *x* direction listed for the anion can be shown[1b] to be pointing along the phenolate groups in the plane of the radical, while the *z* direction is perpendicular to the plane of the radical.

We, therefore, propose that this solvent-broadening effect is due to the production of fixed hydrogen bonds between the alcohol solvent and the semiquinone anion. Hydrogen bonding of this radical at room temperature has been demonstrated to shift both the hyperfine splitting constants[7-13] and the isotropic *g* factor,[14] but does not produce a spectral broadening. In fact, broadening effects are observed only at very low temperatures where the solvent is virtually fixed via hydrogen bonds to the semiquinone radical. At these low temperatures hydrogen bonding is strong enough to allow an electron-nuclear dipole-dipole interaction between the semiquinone's unpaired electron and the alcohol's hydroxyl proton.

The temperature dependency of this hydrogen bonding can be studied quantitatively with the aid of the second moment function. The second moment ($\langle H^2\rangle$) of an ESR spectrum can be written[15] as

$$\langle H^2\rangle = (1/A) \int_{-\infty}^{\infty} (H - H_0)^3 Y' \mathrm{d}H \qquad (1)$$

and is a very sensitive measure of spectral broadening effects. In eq 1, A is the area under the ESR absorption curve obtained by a double integration of the first-derivative ESR spectrum whose amplitude is Y' at each magnetic field value H and whose center occurs at H_0. If the spectrum is sectioned into m identical field increments (ΔH), eq 1 can be expressed as the finite sum

$$\langle H^2\rangle = (\Delta H^2/A) \sum_{j=1}^{m} \sum_{i=j}^{m} (H_j - H_0)^2 Y_i' \qquad (2)$$

The second moments of the various spectra described in the text were calculated using eq 2 along with digitized amplitude points. It has been shown[16,17] that the second moment of an inhomogeneously broadened spectrum is equal to the sum of the second moments of the various broadening factors, e.g., overlapping hyperfine components, anisotropic terms. In our system one factor which broadens the spectrum is the radical-solvent interaction through hydrogen bonding. In fact, this is the only broadening factor of this complex which will be affected by substitution of a deuterated solvent for a protonated solvent. Therefore, the change in the spectrum's second moment upon changing the solvent can be related completely to this interaction. If we define the function δ as

$$\delta = (\langle H^2(T)\rangle_{n\mathrm{h}} - \langle H^2(T)\rangle_{n\mathrm{d}})/(\langle H^2\rangle_{n\mathrm{h}} - \langle H^2\rangle_{n\mathrm{d}})$$

then δ represents the fraction of radicals hydrogen bonded to the solvent as a function of the temperature (T). $\langle H^2\rangle_{n\mathrm{h}}$ and $\langle H^2\rangle_{n\mathrm{d}}$ in the denominator of this expression are the second moments of the completely immobilized semiquinone in protonated and deuterated solvents, respectively, and the numerator contains both of these second moments at a temperature T. As hydrogen bonds are formed, the spectrum will broaden and δ will change from 0 to 1. In Figure 3, δ is plotted for the deuterated semiquinone from −110 to −140 °C. This plot shows that solvent-broadening effect first becomes important at temperatures below −120 °C, which is also the temperature region where the rigid methanol matrix starts to form and hydrogen bonds become fixed in the complexes.

Table I lists the relative second moment of the immobilized semiquinone in selectively deuterated solvents and shows that over half the spectral narrowing effect occurs upon deuteration of the alcohol's hydroxyl proton. As would be expected, this implies that hydrogen bonding of the solvent to the semiquinone is through the hydroxyl proton, or I.

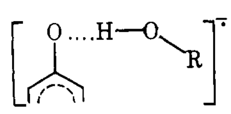

I

Now that hydrogen bonding has been shown to exist in these systems, questions concerning the geometry and structure of these hydrogen-bonded complexes arise. In order to answer the question on structure, it is most helpful to propose three different models for various amounts of solvent-quinone bonding. If we assume that hydrogen bonding can occur at one, two, or four sites on the semiquinone, the following structures can be proposed (II-IV). In order to test our models, we must assume

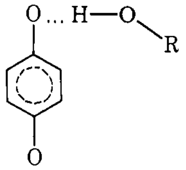

1 site

II

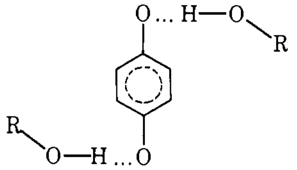

2 sites

III

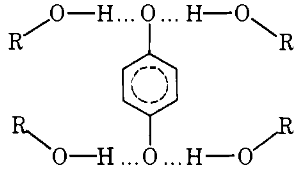

4 sites

IV

further that only one of these models is correct, that the system never exists as a mixture of the various models, and finally, that the same site model exists for the semiquinone in both protonated and deuterated solvents as well as for both protonated and deuterated radicals.

The possibility, of course, exists that these assumptions are not valid and that several different quinone radical species are concurrently frozen into the system. For example, although ion pairing has been shown to not be present in this solvent at room temperature, it may occur at lower temperatures. Since ion pairing is simply an equilibrium process, i.e.,

$$M^+ + Q\cdot^- \rightleftarrows [M^+Q^-]\cdot$$

between a metal cation (M^+) and the semiquinone anion ($Q\cdot^-$), the possible existence of mixtures of $Q\cdot^-$ and the ion pair, $[M^+Q\cdot^-]\cdot$, should be considered. Similarly, hydrogen bonding is also an equilibrium process for each of the different bonding sites, implying the possible presence of a mixture of radicals with differing numbers of hydrogen bonds. Justification for the assumption of a single radical entity bonded to a fixed number of solvent molecules as stated above comes from the experimental facts that the second moment and shape of the semiquinone's powder spectrum are independent of the type of metal cation present (Table I), the concentration of the metal cation (10^{-4}–10^{-1} M), and the concentration of the semiquinone (10^{-4}–10^{-2} M). If there are various equilibrium processes present, therefore, they must all be shifted in favor of the semiquinone radical hydrogen bonded to a fixed number of solvent molecules in the temperature and concentration ranges used in this experiment.

Accepting the assumptions presented above, the validity of each of the hydrogen bonding models can be determined by recording the spectrum of the semiquinone in solvents of different fractional amounts of deuteration. The structure of the spectra obtained will depend not only on the percentage of deuteration of the solvent, but also on the number of sites for hydrogen bonding. For example, the spectrum recorded for a one-site radical in a hydrogen-bonding solvent that is 50% deuterated will be a composite of the spectra of two species, i.e., one species will have a proton hydrogen bond, the other a deuteron. If we initially assume the absence of an isotope effect, each of these species will be in equal concentration. On the other hand, a two-site radical with equal probability for hydrogen bonding at either site can exist as three different species in a mixed protonated-deuterated solvent. For a four-site radical, there are five possible species. For each model, therefore, the resultant spectrum in a mixed solvent represents an overlap of the spectra of all the allowed species, each weighted according to its probable occurrence. Using this interpretation, spectra can be simulated for each model system as a function of the percent deuteration of the solvent. As explained below, however, it would be difficult, if not impossible, to simulate each of the underlying radical species. Therefore, an assumption must be made concerning the shape of each signal. The fully deuterated semiquinone in both protonated and deuterated solvents yields a single-lined ESR spectrum at X-band frequencies. We can approximate this spectrum as being symmetric with a Gaussian line shape. Obviously this approximation is very poor when trying to describe the shapes of the wings of the spectrum, but very good if one is only concerned with the peak-to-peak line width ($\Delta H_{\text{p-p}}$). The value of $\Delta H_{\text{p-p}}$ for the semiquinone with all hydrogen-bonding sites protonated or deuterated can be extracted from the data (Figure 1) to be 4.0 and 2.2 G, respectively. On the other hand, $\Delta H_{\text{p-p}}$ for the intermediate species with mixtures of proton and deuteron bonding in the two- and four-site models cannot be obtained directly from spectra, since these species are never observed by themselves. With the assumption of a Gaussian line shape, however, $\Delta H_{\text{p-p}}$ can be approximated for these remaining species, again using the fact that the second moment of an ESR signal is equal to the sum of the second moments of all the spectral broadening effects. Line widths can be determined using these calculated second moments, since, for a Gaussian line, $(\Delta H_{\text{p-p}})^2$ is proportional to the second moment.

Figure 4 shows $\Delta H_{\text{p-p}}$ as a function of the percentage of deuteration of the solvent as determined by a computer simulation (solid curves) of the spectra for the three different site models. Experimental data (dots) are also plotted in this figure, where the dashed line represents the best curve fit of the data. It is immediately obvious from this figure that the empirical data is vastly different from the results predicted by the model systems. In fact, it can be easily shown that no multi-site hydrogen-bonding model such as those described above will predict the data shown in Figure 4. The error, however, is not in the model used, but in an assumption incorporated into the theoretical calculation of $\Delta H_{\text{p-p}}$ for various percentages of deuteration. In calculating these line widths, we assumed that

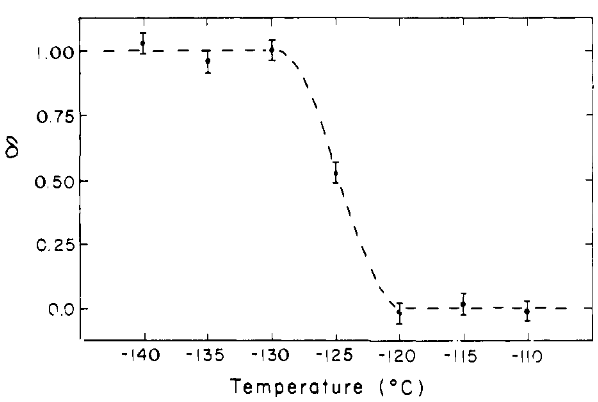

Figure 3. Fractional solvent broadening (δ; see text for definition) of the deuterated semiquinone anion in methanol as a function of temperature. (Measured at X-band; microwave power = 0.1 mW.)

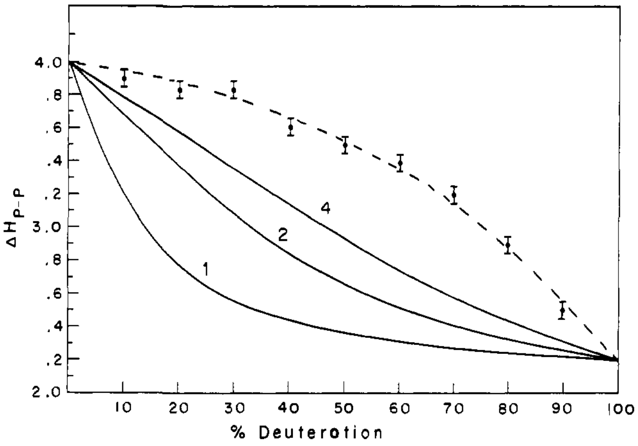

Figure 4. Theoretical (solid lines) and experimental (•) variation of $\Delta H_{p\text{-}p}$ for the deuterated semiquinone anion in methanol at 77 K as a function of percent deuteration of the solvent for one-, two-, and four-site models. Dashed line represents a best-fit calculation of the experimental data.

in a mixed solvent the probability of deuterium bonding at each site in the radical is equal to the percentage of deuteration of the solvent, i.e., no isotope effect. In other words, if QHR and QDR represent the semiquinone hydrogen bonded at a single site in protonated and deuterated solvents, respectively, and RH and RD represent molecules of those solvents, then the solid lines in Figure 4 were calculated on the assumption that the exchange reaction

$$\mathrm{QDR} + \mathrm{RH} \overset{K}{\rightleftharpoons} \mathrm{QHR} + \mathrm{RD} \qquad (3)$$

has an equilibrium constant (K) equal to one. Since isotope effects have been observed in numerous exchange reactions, this assumption is, of course, erroneous. For example, stronger protonated than deuterated hydrogen bonds will make K in eq 3 greater than unity or, in other words, the QHR/QDR concentration ratio will be greater at each percent deuteration than was calculated assuming $K = 1$. With this assumption the spectrum of a specified site model will experimentally have a given line width at a higher percent deuteration ($(\mathrm{pD})_{\mathrm{expt}}$) than was calculated ($(\mathrm{pD})_{\mathrm{calcd}}$) from the theoretical model described above. If we assume that each site in the two- and four-site models has the same equilibrium constant, then it can be easily shown (see Appendix I) that

$$(100/\mathrm{pD})_{\mathrm{calcd}} = K(100/\mathrm{pD})_{\mathrm{expt}} + (1 - K) \qquad (4)$$

In order to plot eq 4 to determine K for the different site models, the data in Figure 4 must be used. An example of such a calculation is as follows. The calculated curve (i.e., assuming $K = 1$) for a one-site model shows that a 10% deuteration (i.e., $(\mathrm{pD})_{\mathrm{calcd}} = 10$) $\Delta H_{p\text{-}p} = 3.20$ G. The experimental data show that this $\Delta H_{p\text{-}p}$ does not occur until 74% deuteration (i.e., $(\mathrm{pD})_{\mathrm{expt}} = 74$). Dividing these numbers into 100 yields $(100/\mathrm{pD})_{\mathrm{calcd}} = 10$ and $(100/\mathrm{pD})_{\mathrm{expt}} = 1.35$. Plotting $(100/\mathrm{pD})_{\mathrm{expt}}$ vs. $(100/\mathrm{pD})_{\mathrm{calcd}}$ for the three different site models produces straight lines, as shown in Figure 5. The slope and intercept of each of these were determined by a least-squares analysis of the data and are listed in Table II. The reason why each of these models produces a straight line in Figure 5 instead of only the correct model is not known, but it is obvious from this fact alone that the correct model cannot be identified using only the basis of the linearity of eq 4.

In order to identify unequivocally the number of sites of hydrogen bonding on the immobilized semiquinone another spectral parameter, the second moment, must be employed. Unlike $\Delta H_{p\text{-}p}$, the second moment of the semiquinone in mixed protonated–deuterated solvent depends only on the percentage of deuteration and not on the number of sites for hydrogen bonding (see Appendix II). Because of this property, the second moment observed for a given amount of deuteration can be related to the equilibrium constant of eq 3, independent of any assumptions on the amount of hydrogen bonding in the system. In fact, if we define

$$\alpha = (\langle H^2\rangle_{nd} - \langle H^2\rangle_{nh})/(\langle H^2(\mathrm{pD})\rangle_n - \langle H^2\rangle_{nh})$$

to be the reciprocal of the relative charge in the second moment, where $\langle H^2(\mathrm{pD})\rangle_n$ is the empirical second moment of the semiquinone spectrum at a given percent deuteration of the solvent, then it can be easily shown (Appendix II) that

$$\alpha = K(100/\mathrm{pD})_{\mathrm{expt}} + (1 - K)$$

α's have been calculated from the mixed solvent spectra and are plotted against $(100/\mathrm{pD})_{\mathrm{expt}}$ in Figure 5. Since the α values lie closest to the data for the two-site model, this must be the form of hydrogen bonding in this system.

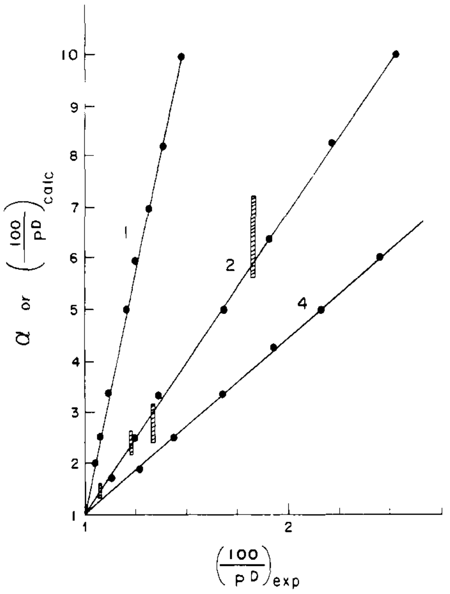

Figure 5. Variation of α (rectangles) and $(100/\mathrm{pD})_{\mathrm{calcd}}$ (dots) as a function of $(100/\mathrm{pD})_{\mathrm{expt}}$ for one-, two-, and four-site models. Solid lines represent least-squares fit of data.

Table II. Least-Squares Analysis of Data in Figure 5

Model	Slope (K)	1 − intercept (K)
1 site	24.6 ± 0.3	26.2 ± 0.3
2 sites	5.8 ± 0.1	5.7 ± 0.2
4 sites	3.5 ± 0.2	3.5 ± 0.2

Discussion

Several important results can be extracted from the data presented in this paper: (1) hydrogen bonding can be directly observed in the ESR spectrum of the semiquinone in rigid media; (2) hydrogen bonds become fixed to the semiquinone radical below ca. −120 °C; (3) computer simulations can be used to determine $\Delta H_{p\text{-}p}$ as a function of the percent deuteration of the solvent for various theorized site models of hydrogen bonding; (4) the equilibrium constant for hydrogen bonding of the semiquinone radical in methanol at temperatures just above freezing is $K = 5.8$ in favor of protonated over deuterated bonds, where the bonding occurs at two equivalent sites on the radical; (5) the second moment of composite spectra in mixed solvents can be used with empirical line widths to yield information concerning both the magnitude of the hydrogen-bonding equilibrium constant and the correct numbers of sites for this bonding.

It is interesting to note that the analysis of the semiquinone spectrum at various percentages of deuteration not only yields information concerning hydrogen bonding as described above, but also shows that this spectrum is not due to the overlap of two different radical species as proposed by Harbour and Tollin.[2] For a system where two radical species are present, i.e., a semiquinone and solvent radical, the dependency of $\Delta H_{\text{p-p}}$ on the percentage of deuteration would mimic closest the one-site theoretical curve. Furthermore, the second moment of such a system would vary according to the theoretical model with $K = 1$. Since neither the one-site nor $K = 1$ properties exist for our system, the spectra described above are clearly not due to overlapping of different radical signals.

Studies of hydrogen bonding of semiquinones using ESR spectroscopy have been completely devoted to the study of solution spectra of the radical in mixed protic-aprotic solvents. Gendell et al.[8] and Stone and Maki[9] hypothesized two-site models for hydrogen bonding of the semiquinone in order to interpret variations in hyperfine splitting constants in these solvents. Yonezawa et al.,[14] on the other hand, suggested a four-site model to describe g factor variation, where the third and fourth bonding sites have weaker hydrogen bonds than the first two. Our data is the most quantitative and clearly implies a two-site model. The equilibrium constant determined for this study refers to the system at a temperature just above the freezing point of methanol.

In addition to the equilibrium constant and the number of sites for hydrogen bonding, a third important question on the nature of hydrogen bonding is its geometry. Although the directional dependency of hydrogen bonding has not been investigated for semiquinone radicals, it has been studied for various other systems. For example, Morishima et al.[18-20] have suggested the presence of hydrogen bonding to the π-oxygen orbital of the nitroxide radical. On the other hand, Kabankin et al.[21,22] have used NMR and ESR spectroscopy to present a strong argument in favor of hydrogen bonding to the oxygen's nonbonding σ orbital. In fact, Koller and Azman[23] as well as Zhidomirov and Kabankin[22] feel that the N-O···H bond angle may be as great as 180°.

Hydrogen bonding of quinones has been extensively studied in single crystals using both x-ray crystallography and infrared spectroscopy. For all the quinone systems, hydrogen-bond complexing produces carbonyl stretching at lower frequencies.[24] Furthermore, x-ray studies concerned with the stoichiometry of hydrogen bonding consistently show the presence of two bonding sites per quinone. Finally, the C-O···H bond angle for hydrogen bonding of quinones is typically 120°, but may be as little as 90°, as exhibited by several phenol-methyl-substituted quinone systems[25] or as great as 172°, as has been demonstrated for the p-benzoquinone-phloroglucinol complex.[26]

Data related to the orientation of hydrogen bonding to the semiquinone can be extracted from Table I. Hydrogen bonding of the semiquinone's oxygens should perturb the energy levels in the direction of the hydrogen bond relative to the orbitals under nonhydrogen bonding conditions. Similarly, since for this system deuterons form weaker hydrogen bonds than protons, their interaction with the semiquinone's orbitals should be smaller than a proton's interaction. Table I shows that substituting CD_3OD for CH_3OH has its greatest effect on the g factor in the y direction. Since the deviation of g^{yy} from the free-electron g factor is caused primarily by spin-orbit mixing of the oxygen π orbital containing the unpaired electron with the orbitals in the x direction on the oxygen atoms[1b] changes in g^{yy} can be related to changes in the energies of the orbitals in the x direction on the oxygen atom. In other words, the data in Table I suggests that hydrogen bonding occurs with the oxygen σ orbitals, where the bond angle for the C-O···H hydrogen bond is closer to 180° than 90°. Further support for this model of hydrogen bonding has recently come from a study in our laboratory on a directional dependency of spin-lattice relaxation in these systems.

Appendix I

As discussed in the text, the presence of an isotope effect in these systems as depicted by eq 3 hampers our ability to correctly simulate spectral line shapes. Without any knowledge of the magnitude of this effect, one is unable to determine the relative weight that must be associated with each spectral shape used in the simulation of the resultant signal. An equilibrium constant for eq 3 can be determined, however, by first simulating spectra assuming $K = 1$ (Figure 4), then determine the value of K needed to coincide the simulated data with the empirical data. The equilibrium constant for this exchange is defined as

$$K = [\mathrm{QHR}][\mathrm{RD}]/[\mathrm{QDR}][\mathrm{RH}] \qquad (\mathrm{I.1})$$

according to eq 3. In order to develop an equation relating this equilibrium to the empirical data, we must first assume that each site on the radical has the same equilibrium constant. The percentage of deuteration representing the amount of semiquinone hydrogen bonded to deuterated solvent molecules can be calculated from the ESR spectra ($(\mathrm{pD})_{\mathrm{calcd}}$) or

$$(\mathrm{pD})_{\mathrm{calcd}} = ([\mathrm{QDR}]/([\mathrm{QDR}] + [\mathrm{QHR}])) \times 100 \qquad (\mathrm{I.2})$$

Since the solvent is in a much higher concentration than the semiquinone, the percentage of deuteration experimentally used in these systems ($(\mathrm{pD})_{\mathrm{expt}}$) is in terms of the relative amount of deuterated solvent used in preparing the original solution, or

$$(\mathrm{pD})_{\mathrm{expt}} = ([\mathrm{RD}]/([\mathrm{RD}] + [\mathrm{RH}])) \times 100 \qquad (\mathrm{I.3})$$

Equation I.2 can be arranged to

$$(\mathrm{pD}/100)_{\mathrm{calcd}} = [\mathrm{QDR}]/([\mathrm{QDR}] + [\mathrm{QHR}]) \qquad (\mathrm{I.4})$$

where inversion yields

$$(100/\mathrm{pD})_{\mathrm{calcd}} = 1 + ([\mathrm{QHR}]/[\mathrm{QDR}]) \qquad (\mathrm{I.5})$$

or

$$[\mathrm{QHR}]/[\mathrm{QDR}] = (100/\mathrm{pD})_{\mathrm{calcd}} - 1 \qquad (\mathrm{I.6})$$

Equation I.3 can be similarly rearranged to

$$[\mathrm{RH}]/[\mathrm{RD}] = (100/\mathrm{pD})_{\mathrm{expt}} - 1 \qquad (\mathrm{I.7})$$

Separating the solvent- and quinone-dependent portions of eq I.1 yields

$$([\mathrm{RH}]/[\mathrm{RD}])K = [\mathrm{QHR}]/[\mathrm{QHD}] \qquad (\mathrm{I.8})$$

which, after substitution of eq I.6 and I.7 becomes

$$\{(100/\mathrm{pD})_{\mathrm{expt}} - 1\}K = (100/\mathrm{pD})_{\mathrm{calcd}} - 1$$

or

$$(100/\mathrm{pD})_{\mathrm{calcd}} = K(100/\mathrm{pD})_{\mathrm{expt}} + (1 - K) \qquad (\mathrm{I.9})$$

Therefore, as detailed in the text, plotting the reciprocal of the fraction deuteration derived from these spectral calculations ($(100/\mathrm{pD})_{\mathrm{calcd}}$) vs. the reciprocal of the experimentally determined percent deuteration ($(100/\mathrm{pD})_{\mathrm{expt}}$) for a signal line width yields the equilibrium constant (K) as the slope and ($1 - K$) as the intercept.

Appendix II

The second moment ($\langle H^2 \rangle$) of a powder spectrum, which represents a composite of the spectra of several different signals, can be calculated by noting two important properties of this function.

(1) The second moment of an inhomogeneously broadened line is equal to the sum of the second moments of all of the line-broadening factors, e.g., g factor anisotropy, unresolved hyperfine structure, spin relaxation.

(2) The second moment of a spectrum, which is a composite of overlapping signals, is equal to the sum of the second moments of each underlying signal weighted by their relative concentrations.

If one assumes n equivalent sites for hydrogen bonding, the total second moment ($\langle H^2\rangle_{n\mathrm{h}}$) of a spectrum of a radical in a proton containing solvent can be written as

$$\langle H^2\rangle_{n\mathrm{h}} = n\langle H^2\rangle_{\mathrm{h}} + \langle H^2\rangle_{\mathrm{Res}} \tag{II.1}$$

where $\langle H^2\rangle_{\mathrm{h}}$ is the contribution to $\langle H^2\rangle_{n\mathrm{h}}$ from each of the n hydrogen-bonding sites and $\langle H^2\rangle_{\mathrm{Res}}$ is the residual second moment of the spectrum due to all of the remaining line-broadening effects. Similarly, the total second moment in a deuterated solvent ($\langle H^2\rangle_{n\mathrm{d}}$) can be written in terms of $\langle H^2\rangle_{\mathrm{d}}$ for each of the n deuterated sites as

$$\langle H^2\rangle_{n\mathrm{d}} = n\langle H^2\rangle_{\mathrm{d}} + \langle H^2\rangle_{\mathrm{Res}} \tag{II.2}$$

Finally, the second moment of a radical's signal containing ($n - r$) protonated hydrogen bonds and r deuterated hydrogen bonds is

$$\langle H^2\rangle_{(n-r)\mathrm{h},r\mathrm{d}} = (n-r)\langle H^2\rangle_{\mathrm{h}} + r\langle H^2\rangle_{\mathrm{d}} + \langle H^2\rangle_{\mathrm{Res}} \tag{II.3}$$

In a mixed protonated-deuterated protic solvent, various radical species will exist, each corresponding to a radical hydrogen bonded to different numbers of deuterons and protons. For example, a system where the radical contains two equivalent hydrogen-bonding sites will exhibit a spectrum formed by the overlap of three different radical species: one corresponding to the radical possessing two protonated hydrogen bonds, one corresponding to two deuterated hydrogen bonds, and the last corresponding to those radicals where one site has a protonated hydrogen bond and the other a deuterated hydrogen bond, e.g., for semiquinones, see structures **1**–**3**. Each of these species will contribute to the total second moment in proportion to their relative concentration. The relative concentration of a species in a system with no isotope effect is dependent on two factors: (1) the number of equivalent hydrogen-bonded species with identical second moments, which is equal to $n!/(n-r)!r!$, where n equals the total number of bonding sites and r equals the number of sites which are deuterated in that species (e.g., structure **3** above has two equivalent species (**3a** and **3b**), since $n = 2$ and $r = 1$); and (2) the fraction deuteration of the medium ($(\mathrm{pD}/100)_{\mathrm{calcd}}$) as defined by eq I.4. The amount of deuteration of the medium will affect the relative concentration according to the factor

$$(\mathrm{pD}/100)^r[1 - (\mathrm{pD}/100)]^{n-r}$$

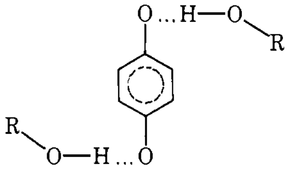

1

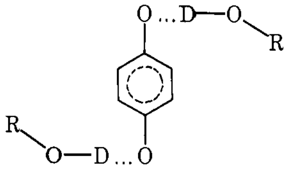

2

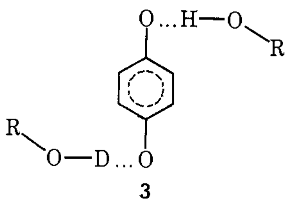

3

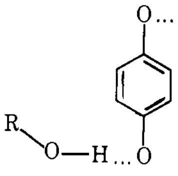

3a

and

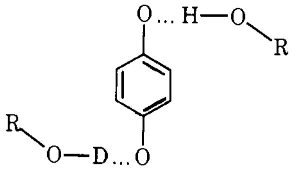

3b

Therefore, the second moment of a spectrum of a radical at a given percent deuteration ($\langle H^2(\mathrm{pD})\rangle_n$) consisting of a composite of hydrogen-bonded signals is a function of both the number of hydrogen-bonding sites (n) and the fraction deuteration of the medium ($(\mathrm{pD}/100)_{\mathrm{calcd}}$) and can be written as a sum of the weighted second moment of each of the underlying signals, or

$$\langle H^2(\mathrm{pD})\rangle_n = \sum_{r=0}^{n} \frac{n!}{(n-r)!r!}\left(\frac{\mathrm{pD}}{100}\right)^r_{\mathrm{calcd}} \times \left[1 - \left(\frac{\mathrm{pD}}{100}\right)_{\mathrm{calcd}}\right]^{n-r} \langle H^2\rangle_{(n-r)\mathrm{h},r\mathrm{d}} \tag{II.4}$$

Substitution of eq II.3 into II.4 yields

$$\langle H^2(\mathrm{pD})\rangle_n = \sum_{r=0}^{n} \frac{n!}{(n-r)!r!}\left(\frac{\mathrm{pD}}{100}\right)^r_{\mathrm{calcd}} \times \left[1 - \left(\frac{\mathrm{pD}}{100}\right)_{\mathrm{calcd}}\right]^{n-r} [(n-r)\langle H^2\rangle_{\mathrm{h}} + r\langle H^2\rangle_{\mathrm{d}} + \langle H^2\rangle_{\mathrm{Res}}]$$

Since n, $\langle H^2\rangle_{\mathrm{h}}$, $\langle H^2\rangle_{\mathrm{d}}$, and $\langle H^2\rangle_{\mathrm{Res}}$ are constants defined by the system and are not functions of r,

$$\langle H^2(\mathrm{pD})\rangle_n = (n\langle H^2\rangle_{\mathrm{h}} + \langle H^2\rangle_{\mathrm{Res}}) \sum_{r=0}^{n} \frac{n!}{(n-r)!r!} \times \left(\frac{\mathrm{pD}}{100}\right)^r_{\mathrm{calcd}} \left[1 - \left(\frac{\mathrm{pD}}{100}\right)_{\mathrm{calcd}}\right]^{n-r} + (\langle H^2\rangle_{\mathrm{d}} - \langle H^2\rangle_{\mathrm{h}}) \times \sum_{r=0}^{n} \frac{n!r}{(n-r)!r!}\left(\frac{\mathrm{pD}}{100}\right)^r_{\mathrm{calcd}} \left[1 - \left(\frac{\mathrm{pD}}{100}\right)_{\mathrm{calcd}}\right]^{n-r} \tag{II.5}$$

According to eq II.1, the coefficient of the first sum is $\langle H^2\rangle_{n\mathrm{h}}$, the second moment of the radical in a totally protonated solvent. Furthermore, the first sum is actually a binomial expansion of the form

$$\sum_{a=0}^{b} (b!/(b-a)!a!)x^a y^{b-a} = (x+y)^b$$

Since for our system $x = (\mathrm{pD}/100)_{\mathrm{calcd}}$ and $y = [1 - (\mathrm{pD}/100)_{\mathrm{calcd}}]$, the first sum in eq II.5 equals unity.

Accordingly, the second sum in eq II.5 can be rewritten as

$$n\left(\frac{\mathrm{pD}}{100}\right)_{\mathrm{calcd}} \sum_{r=0}^{n-1} \frac{(n-1)!}{(n-1-r)!(r)!} \times \left(\frac{\mathrm{pD}}{100}\right)^r_{\mathrm{calcd}} \left[1 - \left(\frac{\mathrm{pD}}{100}\right)_{\mathrm{calcd}}\right]^{n-1-r}$$

which equals $n(\mathrm{pD}/100)_{\mathrm{calcd}}$ since this sum is also unity. Therefore,

$$\langle H^2(\mathrm{pD})\rangle_n = \langle H^2\rangle_{n\mathrm{h}} + n(\langle H^2\rangle_{\mathrm{d}} - \langle H^2\rangle_{\mathrm{h}})(\mathrm{pD}/100)_{\mathrm{calcd}}$$

or

$$\langle H^2(\mathrm{pD})\rangle_n = \langle H^2\rangle_{n\mathrm{h}} + (\langle H^2\rangle_{n\mathrm{d}} - \langle H^2\rangle_{n\mathrm{h}})(\mathrm{pD}/100)_{\mathrm{calcd}} \tag{II.6}$$

Equation II.6 shows that the second moment of a spectrum of a hydrogen bonded molecule varies linearly with the fraction deuteration and does not depend on n, the number of bonding sites.

In order to extend eq II.6 into the consideration of those systems where there exists an isotope effect, eq I.9 derived in Appendix I must be used. If eq II.6 is rewritten as

$$(\langle H^2\rangle_{nd} - \langle H^2\rangle_{nh})/(\langle H^2(\mathrm{pD})\rangle_n - \langle H^2\rangle_{nh}) = (100/\mathrm{pD})_{\mathrm{calcd}} \qquad \text{(II.7)}$$

substitution of eq I.9 yields

$$\alpha = K(100/\mathrm{pD})_{\mathrm{expt}} + (1 - K) \qquad \text{(II.8)}$$

where

$$\alpha = (\langle H^2\rangle_{nd} - \langle H^2\rangle_{nh})/(\langle H^2(\mathrm{pD})\rangle_n - \langle H^2\rangle_{nh})$$

Therefore, plotting α vs. $(100/\mathrm{pD})_{\mathrm{expt}}$ should yield a straight line of slope K and intercept $(1 - K)$. This means that the variation of both the second moment and the spectral line width (see Appendix I) can be used to calculate the proton–deuteron hydrogen-bonding equilibrium constant. The attainment of K by these two nonrelated techniques is highly significant. The use of line widths to determine K requires knowledge of the number of bonding sites. On the other hand, the use of the spectrum's second moment yields K directly, but states nothing about the number of bonding sites. Therefore, both of these techniques are necessary for the unequivocal determination of both the equilibrium constant and the number of hydrogen-bonding sites.

References and Notes

(1) (a) Supported in part by a Cottrell Research Grant from Research Corporation and Grant No. GM23272 by the Public Health Services. (b) First paper in this series: B. J. Hales, *J. Am. Chem. Soc.*, **97**, 5993 (1975).
(2) J. R. Harbour and G. Tollin, *Proc. Natl. Acad. Sci., U.S.A.*, **69**, 2066 (1972).
(3) M. S. Blois, H. W. Brown, R. M. Lemmon, R. O. Lindblom, and M. Weissbluth, Ed., "Free Radicals in Biological Systems", Academic Press, New York, N.Y., 1961.
(4) E. Charney and E. Becker, *J. Chem. Phys.*, **42**, 3314 (1972).
(5) B. J. Hales and J. R. Bolton, *J. Am. Chem. Soc.*, **94**, 3314 (1972).
(6) J. R. Harbour and G. Tollin, *Photochem. Photobiol.*, **19**, 147 (1974).
(7) E. W. Stone and A. H. Maki, *J. Chem. Phys.*, **36**, 1944 (1962).
(8) J. Gendell, J. H. Freed, and G. K. Fraenkel, *J. Chem. Phys.*, **37**, 2832 (1962).
(9) E. W. Stone and A. H. Maki, *J. Am. Chem. Soc.*, **87**, 454 (1965).
(10) M. R. Das and G. K. Fraenkel, *J. Chem. Phys.*, **42**, 1350 (1965).
(11) W. M. Gulick and D. H. Geske, *J. Am. Chem. Soc.*, **88**, 4119 (1966).
(12) M. Broze, Z. Luz, and B. L. Silver, *J. Chem. Phys.*, **46**, 4891 (1967).
(13) W. E. Geiger and W. M. Gulick, *J. Am. Chem. Soc.*, **91**, 4657 (1969).
(14) T. Yonezawa, T. Kawamura, M. Ushio, and Y. Nakao, *Bull. Chem. Soc. Jpn.*, **43**, 1022 (1970).
(15) C. P. Poole, "Electron Spin Resonance. A Comprehensive Treatise on Experimental Techniques", Interscience, New York, N.Y., 1967.
(16) M. W. Hanna, A. D. McLachlan, H. H. Dearman, and H. M. McConnell, *J. Chem. Phys.*, **37**, 361 (1962).
(17) G. Vincow and P. M. Johnson, *J. Chem. Phys.*, **39**, 1143 (1963).
(18) I. Morishima, K. Endo, and T. Yomezawa, *J. Am. Chem. Soc.*, **93**, 2048 (1971).
(19) I. Morishima, K. Endo, and T. Yomezawa, *Chem. Phys. Lett.*, **9**, 143, 203 (1971).
(20) I. Morishima, K. Endo, and T. Yomezawa, *J. Chem. Phys.*, **58**, 3146 (1973).
(21) A. S. Kabankin, G. M. Zhidomirov, and A. L. Bachachenko, *J. Magn. Reson.*, **9**, 199 (1973).
(22) G. M. Zhidomirov and A. S. Kabankin, *J. Magn. Reson.*, **19**, 47 (1975).
(23) J. Koller and A. Azman, *Croat. Chem. Acta*, **42**, 583 (1970).
(24) M. A. Slifkin and R. H. Walmsley, *Spectrochim. Acta, Part A*, **26**, 1237 (1970).
(25) H. Fritzsche, *Z. Phys. Chem.*, **43**, 154 (1964).
(26) T. Sakurai and H. Tagawa, *Acta Crystallogr., Part B*, **27**, 1453 (1971).

---

tert-Butoxycarbonylaminoacyl-4-(oxymethyl)-phenylacetamidomethyl-Resin, a More Acid-Resistant Support for Solid-Phase Peptide Synthesis[1]

A. R. Mitchell,* B. W. Erickson,* M. N. Ryabtsev,[2] R. S. Hodges, and R. B. Merrifield

Contribution from The Rockefeller University, New York, New York 10021.

Received February 24, 1976

Abstract: Some of the peptide chains esterified to the hydroxymethyl-poly(styrene-*co*-divinylbenzene) resin are lost by acidolysis during solid-phase peptide synthesis. This loss has been minimized by using 4-(hydroxymethyl)phenylacetamidomethyl-poly(styrene-*co*-divinylbenzene) as the solid support. The phenylacetamidomethyl (Pam) bridge between the peptide and the resin is sufficiently electron withdrawing that the peptidyl-OCH_2-Pam-resin is 100 times more stable than the conventional peptidyl-OCH_2-resin to cleavage of the ester bond by 50% trifluoroacetic acid in dichloromethane. Boc-Val-OCH_2-Pam-resin, which was prepared by two routes, compared favorably with Boc-Val-OCH_2-resin for synthesis of the model peptides leucylalanylglycylvaline and decalysylvaline. The greater acid stability of the Pam-resin is expected to result in much higher yields of large peptides prepared by solid-phase peptide synthesis.

The solid support commonly used for solid-phase peptide synthesis,[3] *tert*-butoxycarbonylaminoacyloxymethyl-poly(styrene-*co*-divinylbenzene), is not completely stable under the acidic conditions required to remove the *tert*-butoxycarbonyl (Boc) group.[4-7] Acidolysis of the benzyl ester link between a peptide acid and the hydroxymethyl-resin is undesirable during stepwise assembly of the peptide because the yield of crude peptide obtained at the end of the synthesis is thereby decreased. In addition, the production of new hydroxymethyl sites due to premature release of peptide chains from the resin can result in the late initiation of peptides and formation of deletion peptides lacking one or more residues at the carboxyl terminus. Early acidolysis of peptide chains during solid-phase peptide synthesis can be minimized or prevented by use of a more acid-resistant bond between the peptide and the solid support as described in this paper.

The benzyl ester link has been rendered more resistant to acid by attachment of electron-withdrawing substituents to the benzene ring.[8] This approach was originally described by Merrifield,[3] who nitrated (or brominated) every aromatic ring

Mitchell et al. / Boc-aminoacyl-4-(oxymethyl)phenylacetamidomethyl-Resin